Table 4. Results of cell counts in organising pneumonia

Cell type	Cell count (cells/mm^2)
CD45+ cells, total leucocytes	989.5±154.6 (688–1,268)
CD68+ cells, macrophages	224.6±125.5 (70–489)
CD4+ cells, CD4+ T lymphocytes	320.6±62.9 (201–470)
CD8+ cells, CD8+ T lymphocytes	432.7±79.5 (332–580)

Values are expressed as mean ± standard deviation (range)

than air-space consolidation. However, air-space consolidation, which was the most frequent finding in our study, was significantly associated with the maximal SUV, suggesting that the fusion of ^{18}F-FDG PET and CT images may be useful for evaluating disease activity in patients with organising pneumonia.

Müller et al. [9] concluded that air-space consolidation identified on CT images was correlated with the presence of disease activity, as indicated by a histopathological analysis of specimens from patients with bronchiolitis obliterans with organising pneumonia (BOOP). Increased ^{18}F-FDG accumulation was strongly correlated with disease activity in patients with BOOP [21]. As well as patients with organising pneumonia, which included a variety of inflammatory states of the lung in the present study, patients with infections, pneumoconiosis and tuberculosis can be expected to have positive ^{18}F-FDG PET results [18]. While, increased ^{18}F-FDG uptake during pulmonary inflammation is considered to be a non-specific finding, this measure often reflects disease activity or severity. Thus, the combination of ^{18}F-FDG PET and CT images may be useful for indicating the regional active inflammation in patients with organising pneumonia, but not as a diagnostic test for the disease.

In our study, PET measurements of all patients were shown to be significantly depressed after recovery from organising pneumonia. Therefore, it can be postulated that evaluation of PET measurements may reflect disease activity in patients with organising pneumonia. Patients with organising pneumonia often receive steroids for extended periods, and ^{18}F-FDG accumulation may be the sign of choice for monitoring disease activity [25]. However, steroid therapy may induce false negative results owing to hyperglycaemia while the underlying condition is still active. Further studies in this field, focussing on the progression of organising pneumonia and the efficacy of therapeutic protocols, are warranted.

One potential bias of the present study is that 18 of the patients with organising pneumonia underwent a transbronchial lung biopsy, whereas the others underwent an open lung biopsy. In open lung biopsies, the surgeon selects the lesion to be biopsied, and this may have influenced the results by exaggerating the differences in inflammatory cells between the two groups. However, if this was the case, the difference in inflammatory cells would be even greater between two better matched groups of patients, thus confirming that the findings of an enhanced inflammatory response in organising pneumonia are valid. Another potential bias of this study is that the co-registration of PET and CT images has a limited performance. Misregistration can be caused by body motion related to respiration, cardiovascular pulsation and patient movement, which is averaged over a relatively long time. Further studies using respiratory-gated PET/CT image fusion techniques to reduce the effect of misregistration are needed.

In conclusion, patients with organising pneumonia have an enhanced ^{18}F-FDG accumulation within their lesions compared with normal subjects. The increased numbers of CD45$^+$ cells and CD8$^+$ T lymphocytes in parenchymal lesions are associated with air-space consolidation on PET/CT fused images, reflecting the degree of disease activity.

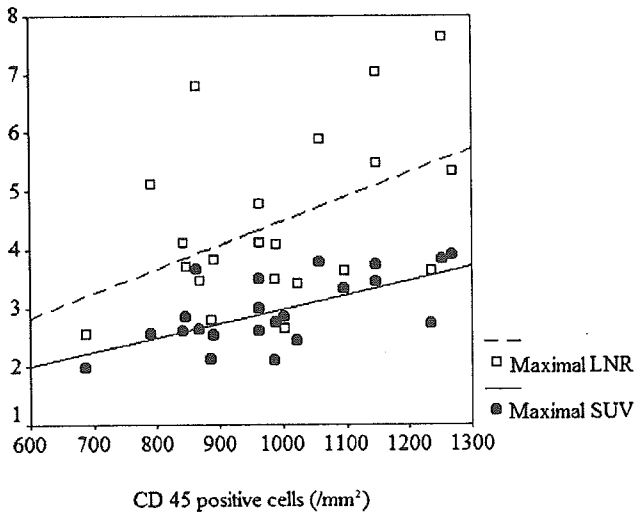

Fig. 2. Relationship between the number of total leucocytes (CD45$^+$ cells) and maximal SUV (•) or maximal LNR (□)

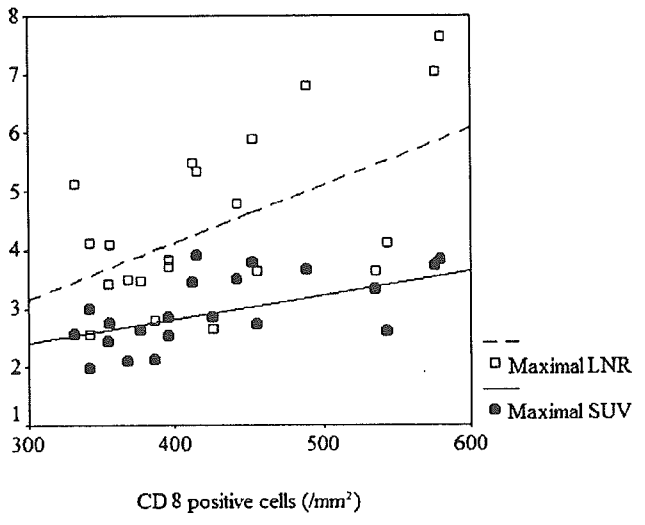

Fig. 3. Relationship between the number of CD8$^+$ T lymphocytes infiltrating the lesion and maximal SUV (•) or maximal LNR (□)

Acknowledgements. This work was supported in part by grants for Scientific Research Expenses for Health and Welfare Programs, No. 17–12, "The promotion and standardization of diagnostic accuracy in PET-CT imaging of lung cancer".

References

1. Epler GR, Colby TV, McLoud TC, Carrington CB, Gaensler EA. Bronchiolitis obliterans organizing pneumonia. N Engl J Med 1985;312:152–158
2. Yousem SA, Lohr RH, Colby TV. Idiopathic bronchiolitis obliterans organizing pneumonia/cryptogenic organizing pneumonia with unfavorable outcome: pathologic predictors. Mod Pathol 1997;10:864–871
3. Cordier JF, Loire R, Brune J. Idiopathic bronchiolitis obliterans organizing pneumonia. Definition of characteristic clinical profiles in a series of 16 patients. Chest 1989;96:999–1004
4. Cordier JF. Organizing pneumonia. Thorax 2000;55:318–328
5. Siddiqui MT, Garrity ER, Husain AN. Bronchiolitis obliterans organizing pneumonia-like reactions: a nonspecific response or an atypical form of rejection or infection in lung allograft recipients? Hum Pathol 1996;27:714–719
6. Crestani B, Valeyre D, Roden S, Wallaert B, Dalphin JC, Cordier JF. Bronchiolitis obliterans organizing pneumonia syndrome primed by radiation therapy to the breast. The Groupe d'Etudes et de Recherche sur les Maladies Orphelines Pulmonaires (GERM"O"P). Am J Respir Crit Care Med 1998;158:1929–1935
7. Douglas WW, Tazelaar HD, Hartman TE, Hartman RP, Decker PA, Schroeder DR, et al. Polymyositis-dermatomyositis-associated interstitial lung disease. Am J Respir Crit Care Med 2001;164:1182–1185
8. Ohnishi H, Yokoyama A, Yasuhara Y, Watanabe A, Naka T, Hamada H, et al. Circulating KL-6 levels in patients with drug induced pneumonitis. Thorax 2003;58:872–875
9. Müller NL, Staples CA, Miller RR. Cryptogenic organizing pneumonia: CT findings in 14 patients. Am J Roentogenol 1990;154:983–987
10. Nishimura K, Itoh H. High-resolution computed tomographic features of bronchiolitis obliterans organizing pneumonia. Chest 1992;102:26–31
11. Oikonomou A, Hansell DM. Organizing pneumonia: the many morphological faces. Eur Radiol 2002;12:1486–1496
12. Murphy JM, Schnyder P, Verschakelen J, Leuenberger P, Flower CD. Linear opacities on HRCT in bronchiolitis obliterans organising pneumonia. Eur Radiol 1999;9:1813–1817
13. Ujita M, Renzoni EA, Veeraraghavan S, Well AU, Hansell DM. Organizing pneumonia: perilobular pattern at thin-section CT. Radiology 2004;232:757–761
14. Akira M, Sakatani M, Hara H. Thin-section CT findings in rheumatoid arthritis-associated lung disease: CT patterns and their courses. J Comput Assist Tomogr 1999;23:941–948
15. Kim SJ, Lee KS, Ryu YH, Yoon YC, Choe KO, Kim TS, et al. Reversed halo sign on high-resolution CT of cryptogenic organizing pneumonia: diagnostic implications. Am J Roentgenol 2003;180:1251–1254
16. Kapucu LO, Meltzer CC, Townsend DW. Fluorine-8-fluorodeoxyglucose uptake in pneumonia. J Nucl Med 1998;39:1267–1269
17. Lowe VJ, Hoffman JM, DeLong DM, Patz EF, Coleman RE. Semiquantitative and visual analysis of FDG-PET images in pulmonary abnormalities. J Nucl Med 1994;35:1771–1776
18. Alavi A, Gupta N, Alberini JL, Hickeson M, Adam LE, Bhargava P, et al. Positro emission tomography imaging in nonmalignant thoracic disorders. Semin Nucl Med 2002;32:293–321
19. Bakheet SM, Saleem M, Powe J, Amro AA, Larsson SG, Mahassin Z. F-18 fluorodeoxyglucose chest uptake in lung inflammation and infection. Clin Nucl Med 2000;25:273–278
20. Ichiya Y, Kuwabara Y, Sasaki M, Yoshida T, Akashi Y, Murayama S, et al. FDG-PET in infectious lesions: the detection and assessment of lesion activity. Ann Nucl Med 1996;10:185–191
21. Shin L, Katz DS, Yung E. Hypermetabolism on F-18 FDG PET of multiple pulmonary nodules resulting from bronchiolitis obliterans organizing pneumonia. Clin Nucl Med 2004;29: 654–656
22. Majeski EI, Harley RA, Bellum SC, London SD, London L. Differential role for T cells in the development of fibrotic lesions associated with reovirus 1/L-induced bronchiolitis obliterans organizing pneumonia versus acute respiratory distress syndrome. Am J Respir Cell Mol Biol 2003;28:208–217
23. Kubota R, Yamada S, Kubota K, Ishiwata K, Tamahashi N, Ido T. Intratumoral distribution of fluorine-18-fluorodeoxyglucose in vivo: high accumulation in macrophages and granulation tissues studied by microautoradiography. J Nucl Med 1992;33:1972–1980
24. Mukae H, Kadota J, Kohno S, Matsukura S, Hara K. Increase of activated T-cells in BAL fluid of Japanese patients with bronchiolitis obliterans organizing pneumonia and chronic eosinophilic pneumonia. Chest 1995;108:123–128
25. Oymak FS, Demirbas HM, Mavili E, Akgun H, Gulmez I, Demir R, et al. Bronchiolitis obliterans organizing pneumonia. Clinical and roentgenological features in 26 cases. Respiration 2005;72:254–262

ORIGINAL ARTICLE

Diagnosis of Complete Response to Neoadjuvant Chemotherapy Using Diagnostic Imaging in Primary Breast Cancer Patients

Takashi Kanazawa, MD,* Sadako Akashi-Tanaka, MD,* Eriko Iwamoto, MD,* Miyuki Takasugi, MD,* Tadahiko Shien, MD,* Takayuki Kinoshita, MD,* Kunihisa Miyakawa, MD,† Chikako Shimizu, MD,‡ Masashi Ando, MD,‡ Noriyuki Katsumata, MD,‡ Yasuhiro Fujiwara, MD,‡ and Takashi Fukutomi, MD*

**Division of Surgical Oncology, †Department of Diagnostic Radiology, and ‡Division of Breast and Medical Oncology, National Cancer Center Hospital, Tokyo, Japan*

■ **Abstract:** Advances in the therapeutic agents used for neoadjuvant chemotherapy (NAC) have recently achieved higher response rates and induced a greater number of pathologic complete responses (pCR) than ever before. The aim of this study is the diagnosis of pCR after NAC by diagnostic imaging of clinical complete response (cCR) patients. This study included 35 breast cancer patients who demonstrated cCR after receiving NAC with a combination of anthracycline and taxane from May 1998 to August 2003. Surgical treatment included breast-conserving therapy followed by radiotherapy or mastectomy. The identity of post-NAC lesions as either a complete response (CR) or partial response (PR) were made by mammography, ultrasonography, and contrast-enhanced computed tomography (CT). Among the 35 patients, 11 achieved pCR, including the disappearance of both invasive and intraductal components. Of the patients achieving pCR, eight were defined as CR and three were determined to be PR by CT. There was a significant relationship between the pCR and the determination of CR by CT. The determination of CR by ultrasonography was indicative of the disappearance of pathologic invasive components. While mammography appeared to reflect the observed histologic results, we did not observe any statistical differences. A subset of cases exhibited discrepancies between the imaging and pathologic results, likely due to the replacement of destroyed tumor cells by fibrosis and granulomatous tissue. The evaluation of CR by CT was significantly indicative of pCR. The positive predictive value, however, was not large enough to avoid surgical treatment. Further studies will be needed to establish a diagnosis of pCR. ■

Key Words: breast cancer, complete response, computed tomography, diagnostic images, neoadjuvant chemotherapy

With advances in the therapeutic agents and combinations used for neoadjuvant chemotherapy (NAC), we have recently achieved higher response rates and greater numbers of pathologic complete responses (pCR). Until now, the highest rate of pCR reported was 66% (1). The accurate evaluation of the existence of residual disease after NAC would facilitate more effective strategies for local treatment after NAC.

We previously reported the efficacy of contrast-enhanced computed tomography (CT) as a method to determine the extent of residual breast cancer following NAC (2). Multiple reports have also demonstrated the accuracy of magnetic resonance imaging (MRI) in the detection of residual breast cancer after NAC (3,4). However, these studies utilized only a small number of pCR cases and did not describe the specific findings of the pCR images. To our knowledge, only a few reports detailing the diagnostic findings for patients with clinical complete responses (cCR) have been published (5,6); these suggest the accuracy of breast CT or MRI for precise evaluation of pCR. This study sought to diagnose pCR precisely after NAC by diagnostic imaging of cCR patients.

Address correspondence and reprint requests to: Sadako Akashi-Tanaka, MD, Breast Surgery Division, National Cancer Center Hospital, 5-1-1 Tsukiji, Chuo-ku, Tokyo 104-0045, Japan, or e-mail: sakashi@gan2.ncc.go.jp.

The Breast Journal, Volume 11 Number 5, 2005 311–316

MATERIALS AND METHODS

Patients

A total of 202 women with pathologically confirmed breast carcinomas measuring more than 3 cm in diameter were eligible for NAC at the National Cancer Center Hospital (NCCH), Tokyo, Japan, from May 1998 to August 2003. This study examined 35 patients who obtained cCR

Table 1. Chemotherapy Regimen

Regimen	Treatment period	Number of patients
ADM (50 mg/m^2), DTX (60 mg/m^2) × 4	98.5–2001.8	26
ADM (60 mg/m^2), CPA (600 mg/m^2) × 4 PTX (80 mg/m^2) × 12 weeks[a]	2002.3–2005	4
5FU (500 mg/m^2), EPI (100 mg/m^2), CPA (500 mg/m^2) × 4, PTX (80 mg/m^2) × 12 weeks[a]	2002.10–2003.8	5

ADM, adriamycin; CPA, cyclophosphamide; DTX, docetaxel; EPI, epirubicin; 5FU, 5-fluorouracil; PTX, paclitaxel.
[a]Trastuzumab was added when the tumor showed overexpression of HER-2.

after NAC followed by local treatment. Inflammatory breast carcinomas were excluded from this study. All patients gave informed consent for study participation as approved by the institutional review board of NCCH. Of the 167 non-cCR patients, pCR was achieved in 7 cases. These cases were not examined in this study. Responses were assessed before and after NAC by clinical measurement by palpation of the primary tumor. The response was determined according to the criteria of the International Union Against Cancer (7). cCR was defined as total resolution of the breast mass by physical examination without considering the result of diagnostic imaging.

Treatment

The presence of a breast carcinoma was confirmed pathologically by core needle biopsy (CNB). The NAC regimen employed a combination of anthracycline and taxane (Table 1). Patients underwent surgical treatment, including modified radical mastectomy or breast-conserving therapy (BCT) approximately 4 weeks after the last NAC cycle. BCT was followed by radiotherapy to achieve a total dose of 50 Gy. When margin was involved by cancer cells, we added a radiation boost to the tumor bed.

Imaging Examinations

Mammography, ultrasonography, and CT were examined before and after NAC, as reported previously (8). CT scans were performed using a helical CT scanner (X-vigor, Toshiba Medical Systems, Tokyo, Japan) before 2002 and a multislice helical CT scanner (Aquilion 4, Toshiba Medical Systems) at a current of 200 mA after 2002. Patients underwent a single spiral acquisition during inspiratory apnea for 30 seconds in the supine position. An enhanced CT scan was performed for the whole breast using a slice thickness of 1 mm with 100 ml of nonionic contrast material injected into the patient at a rate of 3 ml/second. After 40 seconds of bolus (2) administration of contrast material, we began early phase scanning. The late-phase scan was performed 3 minutes after administration. Using a Mammomat 3000 (Siemens, Malvern, PA), craniocaudal and mediolateral mammography views were obtained without magnification. Breast ultrasound images were obtained using a SSA340A (Toshiba Medical Systems). We measured the diameter of tumor in the transverse plane with all modalities.

The responses to NAC in the obtained images were classified as complete response (CR) and partial response (PR) (Fig. 1). By mammography, we defined CR as the absence of a mass and spiculation, while PR was when an obvious mass was observed. In the absence of tumor shadows, microcalcifications were classified as PR (Iwamoto E, et al., personal communication). Three cases could not

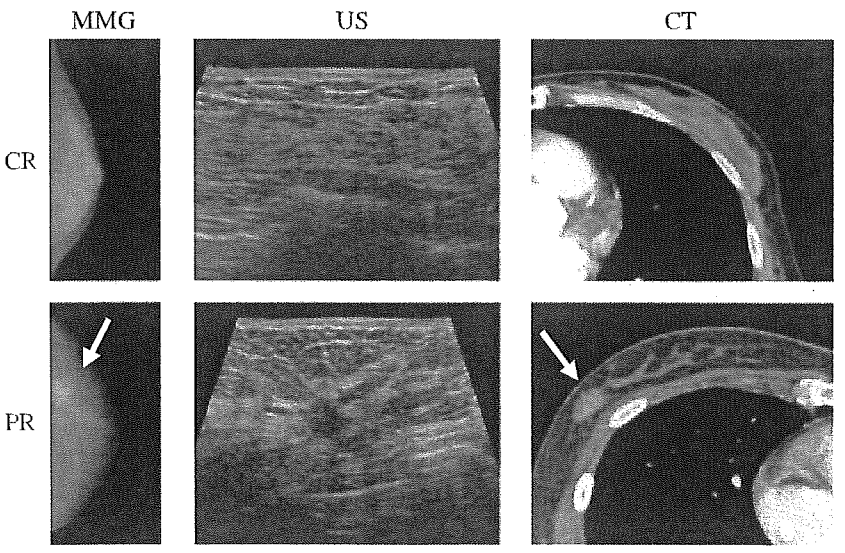

Figure 1. Typical CR and PR determined by each imaging modality.

be evaluated because of the density of the breast. By ultrasonography, a diagnosis of CR was made when the ultrasound findings were normal and PR when images exhibited low echoic lesions with lower echoes than fat tissue or obvious masses. By CT, we defined CR as the complete absence of marks or small and faint enhanced lesions, which were diagnosed as mastopathy when the original tumor location was unknown. CT findings were classified as PR when the images exhibited a highly enhanced mass, regardless of size, or a well-recognized mass, regardless of the enhancement. We classified the tumors into localized and diffuse types by diagnostic imaging, as reported previously (8).

Images were evaluated independently by at least two doctors. Cases without coincident interpretation were mutually agreed upon following discussion.

Histopathologic Examinations

After sectioning in 7–10 mm slices along the transverse axis, all specimens were analyzed by breast pathologists. The response to NAC was classified as either pCR or pathologic partial response (pPR). When neither invasive nor intraductal cancer cells could be observed pathologically, samples were classified as pCR. When residual invasive or noninvasive components were observed, specimens were classified as pPR.

Statistical Analysis

The chi-square test was used for the comparison of CR and PR classifications. Differences of $p < 0.05$ were considered to be significant. Fisher's exact test was used for the comparison when zero was included.

RESULTS

The characteristics of the 35 CR patients are detailed in Table 2. The mean age of the patients obtaining cCR was 48.3 years (range 26–67 years). BCT was performed in 25 cases (71%). Eleven cases (31%) achieved pCR. Twenty-four cases (69%) demonstrated pPR. The determination of histologic type after surgical treatment (pCR cases were diagnosed before NAC by CNB) revealed that 28 cases were diagnosed as invasive ductal carcinoma and 7 were determined to be intraductal carcinoma. Of the seven intraductal carcinomas, six were diagnosed as invasive ductal carcinoma in CNB before NAC. The invasive components were likely diminished by NAC administration.

Tumor sizes were measured before and after NAC on each image (Table 3). The mean tumor size before treatment ranged from 3 cm to 4 cm, diminishing in size to 1–2 cm following NAC. We did not observe a significant difference between the pathologic responses and the sizes obtained at each examination. The mean pathologic sizes were 2.2 cm in pPR patients and 0 cm in pCR patients.

Table 2. Patient's Characteristics

Age (years)	48.3 (26–67)
Menopausal status	
Premenopausal	17 (49%)
Postmenopausal	18 (51%)
Tumor size (before NAC)	4.7 cm (3.2–6.5 cm)
TNM category	
T2	29 (83%)
T3	4 (12%)
T4	2 (6%)
Stage before NAC	
IIA	18 (51%)
IIB	13 (37%)
IIIA	2 (6%)
IIIB	2 (6%)
Local treatment	
Mastectomy	10 (29%)
BCT	25 (71%)
Pathologic response to NAC	
Pathologic PR	24 (69%)
Pathologic CR	11 (31%)

The responses to NAC were evaluated by each imaging method (Table 4). By CT, eight cases were defined as CR and three were determined to be PR in the pCR group. We observed a significant correlation between pCR and the determination of CR by CT ($p < 0.05$). The positive predictive value of CT diagnosis of pCR was 53%. Responses evaluated by ultrasonography, however, did not reflect the pathologic results. In the pPR group, the invasive tumor components disappeared in two of three patients with CR determined by ultrasonography. In these patients, residual intraductal carcinomas were revealed pathologically. The diagnosis of CR by ultrasonography predicted the absence of residual invasive components ($p = 0.1$). Both

Table 3. Mean Tumor Size (cm) before and after NAC and Pathologic Response

	Pathologic PR	Pathologic CR
Mammogram		
Before NAC	3.7	3.6
After NAC	1.5	1.5
Ultrasound		
Before NAC	3.8	3.5
After NAC	1.0	1.2
CT		
Before NAC	4.5	4.2
After NAC	1.4	1.6
Pathology	2.2	0

After NAC, all 35 cases were confirmed total resolution of the breast mass by physical examination and defined as cCR

Table 4. Response to NAC by Each Imaging Modality and Pathologic Response

	Pathologic PR	Pathologic CR	*P*-Value
CT			< 0.05
CR	7	8	
PR	17	3	
Ultrasound			N.S
CR	3	3	
PR	21	8	
Mammogram			0.07
CR	0	2	
PR	23	7	
Not evaluated	1	2	

of the patients evaluated as CR by mammography also exhibited pCR.

Of the 35 cCR subjects, 15, 6, and 2 patients were diagnosed as CR by CT, ultrasonography, and mammography, respectively. In each imaging modality, the complete absence of marks was seen in only two patients. With the exception of these patients, in 13 and 4 patients classified as CR by CT and ultrasonography, respectively, the tumor location was barely identifiable, displaying small lesions recognized only when compared to the pre-NAC images, demonstrating that tumor localization could be identified in all patients using previous images in combination with these three imaging modalities.

One case was defined as CR by all three modalities (Fig. 2). Two cases classified as PR by all three imaging techniques achieved pCR. Pathologically, the observed masses consisted primarily of hyline fibrosis and foamy cells (Fig. 3). One case evaluated as CR by two independent images was shown to possess residual invasive components pathologically (Fig. 4).

The relationships between morphologic tumor type determined by CT before NAC and pathologic response are shown in Table 5. In the pCR group, eight tumors were of the localized type, while three were of the diffuse type. The localized type was more likely to achieve pCR than diffuse type (8).

Table 5. Morphologic Tumor Types on CT Before NAC and Pathologic Response

	Pathological PR[a]	Pathologic CR
Tumor type (pretreatment)		
Localized	10	8
Diffuse	12	3

[a]Two cases were excluded because a CT was not performed before chemotherapy.

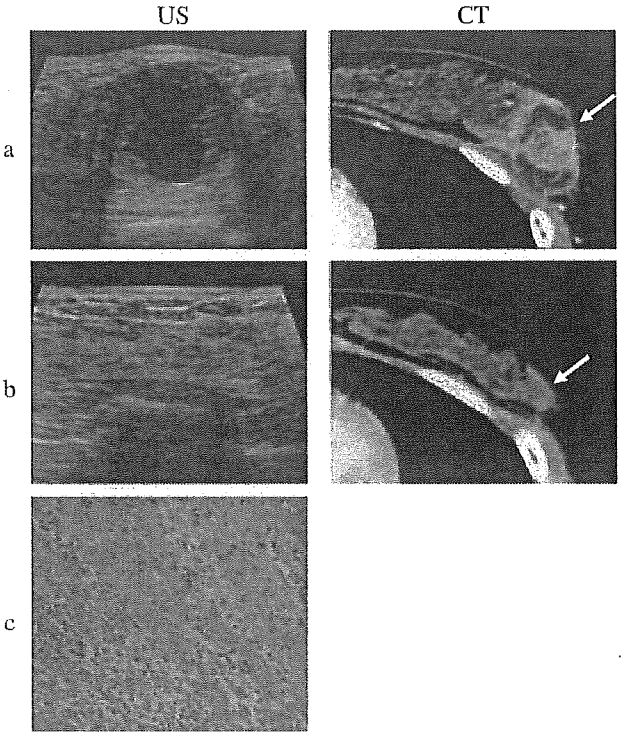

Figure 2. Typical imaging findings for a 30-year-old female with CR. (a) A 5.5 cm × 5.0 cm circumscribed tumor was observed by ultrasonography and CT prior to NAC. (b) After NAC, complete reduction of the tumor was observed by each imaging modality. (c) Subsequent histologic analysis revealed that this case achieved pCR.

DISCUSSION

The determination of CR by CT significantly correlated with pCR. While all tumors or marks could be identified by at least one diagnostic modality to facilitate local excision, tumor size prior to NAC determined by all modalities did not predict pCR, similar to our previous report (2).

This study sought to define CR by diagnostic imaging. Even after the disappearance of all tumor cells, replacement by granuloma-like and/or fibrous tissue could be observed histopathologically. These types of lesions can be identified as low-echoic lesions by ultrasonography and weak-enhanced areas by CT, possibly resulting in false-positive detection of pCR by imaging examination. While these marks provide the important benefit of easy identification of tumor localization when local excision is necessary, the absence of disease signs did not always predict pCR. Of the two tumors lacking any faint shadows or marks identified by ultrasonography, only one achieved pCR. In the false-negative case, we could not distinguish the low-echoic mass surrounded by the aggressive mottled

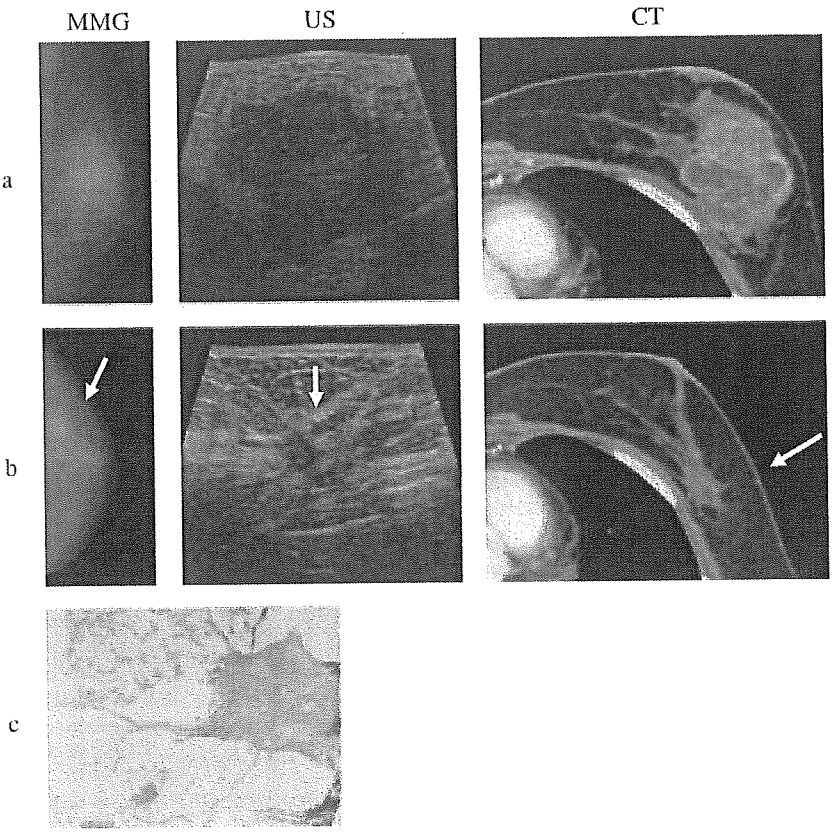

Figure 3. A patient, determined to exhibit PR by imaging, achieved pCR. (a) The localized tumor measured 6.5 cm in size before NAC. (b) After NAC, despite the absence of a palpable tumor, a 1.5 cm localized mass was observed by ultrasonography, CT, and mammography. (c) By histologic analysis, no malignant cells were observed, but hyaline degeneration was seen. This case achieved pCR.

pattern that resulted from fibrocystic changes. Of the two tumors without any enhancement or spiculated marks on CT, neither achieved pCR, instead exhibiting residual intraductal carcinoma. In patients not receiving NAC, the intraductal components of the noncomedo type or low histologic grade demonstrated weaker enhancement than that seen in comedo or high-grade tumors (9,10). These results suggest that low-grade intraductal components may not be well enhanced after NAC, explaining the decreased accuracy of imaging techniques evaluated in this study.

The rate of pCR reported is approximately one-third of the cCR cases (11). Of the few reports examining the role of surgery in patients achieving cCR after NAC, retrospective analysis demonstrated that in patients who achieved cCR after NAC, radiotherapy alone exhibited higher local recurrence rates than surgery (12). These studies suggest that CR defined by residual mass or parenchymal distortion on ultrasonography exhibits better local control in comparison with those lacking ultrasound-detected residual masses. Unfortunately, these patients were not evaluated by mammography, CT, or MRI. While this was not a randomized trial, there were no significant differences in the survival rates following radiotherapy alone or surgery after cCR.

The classification of tumors into either localized or diffuse types using CT prior to NAC administration accurately predicts tumor shrinkage patterns and those tumors that are suitable candidates for BCT following NAC (8). This classification also predicts good pathologic responses (the disappearance of more than two-thirds of tumor cells). Essermann et al. (13) reported similar results using MRI. Of the five predominant MRI patterns, a circumscribed mass pattern significantly predicted good clinical responses to NAC. In this study, localized tumors more frequently achieved pCR. These results were not significant ($p = 0.14$), perhaps because the classification of tumors by diagnostic imaging is a predictor of good pathologic response rather than pCR. The limited number of cases evaluated in these studies, however, requires further evaluation of these imaging techniques as predictors of CR.

In conclusion, CR determined by CT was a significant predictor of pCR. The positive predictive value, however, was not large enough to avoid the necessity of surgical treatment. Further study is required to establish accurately the diagnosis of pCR.

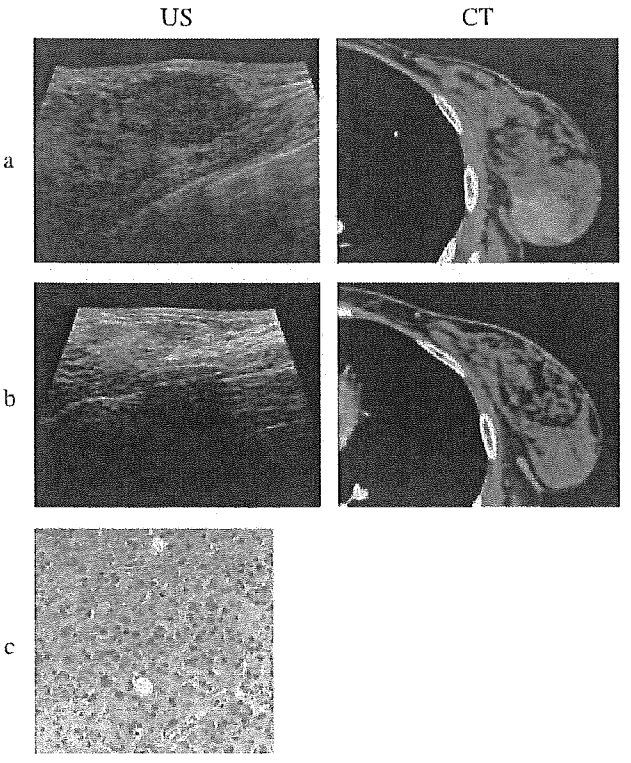

Figure 4. Despite classification as CR by CT and ultrasonography, residual invasive components remained in the specimen by histologic examination. (a) The localized tumor measured 7.5 cm × 3.5 cm in diameter. (b) After NAC, no enhanced lesions were observed by CT. Only a low-echoic area, as low as fat tissue, could be observed by ultrasonography. (c) Invasive components could still be observed histologically.

Acknowledgments

This study was supported in part by a grant-in-aid for cancer research from the Ministry of Health, Labor and Welfare, and a Health and Labor Sciences research grant for research on advanced medical technology (toxicogenomics), Japan.

REFERENCES

1. Buzdar AU, Hunt K, Smith T, *et al.* Significantly higher pathological complete remission (PCR) rate following neoadjuvant therapy with trastuzumab (H), paclitaxel (P), and anthracycline-containing chemotherapy (CT): initial results of a randomized trial in operable breast cancer (BC) with HER/2 positive disease. *J Clin Oncol* 2004;22(July 15 Suppl):520. Abstract.

2. Akashi-Tanaka S, Fukutomi T, Watanabe T, *et al.* Accuracy of contrast-enhanced computed tomography in the prediction of residual breast cancer after neoadjuvant chemotherapy. *Int J Cancer* 2001;96:66–73.

3. Rosen EL, Blackwell KL, Baker JA, *et al.* Accuracy of MRI in the detection of residual breast cancer after neoadjuvant chemotherapy. *Am J Roentgenol* 2003;181:1275–82.

4. Cheung YC, Chen SC, Su MY, *et al.* Monitoring the size and response of locally advanced breast cancers to neoadjuvant chemotherapy (weekly paclitaxel and epirubicin) with serial enhanced MRI. *Breast Cancer Res Treat* 2003;78:51–58.

5. Ogawa Y, Nishioka A, Kubota K, *et al.* CT findings of breast cancer with clinically complete response following neoadjuvant chemotherapy—histological correlation. *Oncol Rep* 2003;10:1411–15.

6. Mumtaz H, Davidson T, Spittle M, *et al.* Breast surgery after neoadjuvant treatment. Is it necessary? *Eur J Surg Oncol* 1996;22:335–41.

7. Therasse P, Arbuck SG, Eisenhauer EA, *et al.* New guidelines to evaluate the response to treatment in solid tumors. *J Natl Cancer Inst* 2000;92:205–16.

8. Akashi-Tanaka S, Fukutomi T, Sato N, *et al.* The use of contrast-enhanced computed tomography before neoadjuvant chemotherapy to identify patients likely to be treated safely with breast-conserving surgery. *Ann Surg* 2004;239:238–43.

9. Akashi-Tanaka S, Fukutomi T, Miyakawa K, Uchiyama N, Tsuda H. Diagnostic value of contrast-enhanced computed tomography for diagnosing the intraductal component of breast cancer. *Breast Cancer Res Treat* 1998;49:79–86.

10. Akashi-Tanaka S, Watanabe T, Fukutomi T, *et al.* Diagnosis of residual breast cancer after neoadjuvant at chemotherapy using contrast-enhanced computed tomography. *J Clin Oncol* 2001;20(May 12 Suppl):1829. Abstract.

11. Fisher B, Bryant J, Wolmark N, Mamounas E, Brown A. Effect of preoperative chemotherapy on the outcome of women with operative breast cancer. *J Clin Oncol* 1998;16:2672–85.

12. Ring A, Webb A, Ashley S, *et al.* Is surgery necessary after complete clinical remission following neoadjuvant chemotherapy for early breast cancer? *J Clin Oncol* 2003;21:4540–45.

13. Esserman L, Kaplan E, Partridge S, *et al.* MRI phenotype is associated with response to doxorubicin and cyclophosphamide neoadjuvant chemotherapy in stage III breast cancer. *Ann Surg Oncol* 2001;8:549–59.

Breast Cancer Research and Treatment (2005) 89: 237–241

Report

Efficacy of weekly paclitaxel in patients with docetaxel-resistant metastatic breast cancer

Kan Yonemori[1], Noriyuki Katsumata[1], Hajime Uno[2], Koji Matsumoto[1], Tsutomu Kouno[1], Shinya Tokunaga[1], Yasuhiro Yamanaka[1], Chikako Shimizu[1], Masashi Ando[1], Masahiro Takeuchi[2], and Yasuhiro Fujiwara[1]

[1]*Breast and Medical Oncology Division, Department of Medical Oncology, National Cancer Center Hospital, 5-1-1 Tsukiji, Chuo-ku;* [2]*Division of Biostatistics, Kitasato University Graduate School, 5-9-1, Shirokane, Minato-ku, Tokyo, Japan*

Key words: docetaxel, metastatic breast cancer, paclitaxel, predictive factor, resistance, taxane

Summary

Background. Partial cross-resistance to paclitaxel and docetaxel has been demonstrated in pre-clinical studies.

Patients and methods. We retrospectively evaluated the efficacy of weekly paclitaxel 80 mg/m^2 in 82 patients with docetaxel-resisitant metastatic breast cancer. Docetaxel resistance was classified into primary resistance, defined as progressive disease while receiving docetaxel, and secondary resistance, defined as progression after achievement of a documented clinical response to docetaxel. Secondary resistance was subclassified according to the interval between the final infusion of docetaxel and the start of weekly paclitaxel into: (1) short interval, $\leqq$120 days, and (2) long interval, >120 days.

Results. The response rate of the 82 patients was 19.5% (95% confidence interval, 10.8–27.9%). The response rate according to the docetaxel resistance category was: primary resistance (n=24), 8.3%; secondary resistance (n=58), 24.1% (short interval [n=39], 17.9%, and long interval, [n=19], 36.8%). The differences in response rates among the three categories were statistically significant (p=0.0247, Cochran–Mantel–Haenszel test). The interval between from the final docetaxel infusion and disease progression were predictors for response of weekly paclitaxel.

Conclusion. Weekly paclitaxel is modestly effective and safe in docetaxel-resistant metastatic breast cancer patients. However, weekly paclitaxel should not be recommended for primary resistance patients with docetaxel.

Abbreviations: MBC: metastatic breast cancer

Introduction

Paclitaxel and docetaxel are currently two of the most effective anticancer drugs in breast cancer chemotherapy [1, 2]. Paclitaxel and docetaxel are the first members of a class of microtubule-stabilizing anticancer agents. They bind to the β-tubulin subunit of the tubulin hetero-dimer, accelerate the polymerization of tubulin, and stabilize the resultant microtubules to inhibit their polymerization. This inhibition results in the arrest of the cell division cycle, mainly at the G2/M2 stage, which triggers the cell signaling cascade, leading to apoptosis of the cancer cells [3–6]. Although the mechanism of action of paclitaxel and docetaxel is similar, there are several notable differences in the way they form stable, non-functional microtubule bundles, and in the affinity of the two compounds for binding sites [7]. Pre-clinical studies have demonstrated docetaxel to be 100-fold more potent than paclitaxel in achieving bcl-2 phosphorylation and apoptotic cell death, and the cellular uptake of docetaxel is greater than that of paclitaxel, both of which lead to greater cytotoxic activity [8, 9]. *In vivo* evidence has suggested the existence of partial cross-resistance between the two drugs despite the fact they share a similar antitumor mechanism [10].

Paclitaxel and docetaxel have shown similar clinical efficacy in patients with anthracyline-resistant metastatic breast cancer (MBC) [1], and the response rate to both was almost the same: 21.5–53% to weekly paclitaxel, and 22.9–57% to docetaxel [10–16].

In retrospective study of Lin et al. observed a response rate of 25% in patients treated with docetaxel at a dose of 75 mg/m^2, who had pre-treated with anthracycline and paclitaxel [17]. In a phase II study Valero et al. observed a response rate of 18.1% in patients with paclitaxel-resistant MBC treated with deocetaxel at a

dose of 100 mg/m^2 infused over 1 h every 3 weeks [18]. These studies suggested partial cross-resistance between paclitaxel and docetaxel [17, 18].

The taxanes, i.e., docetaxel and paclitaxel, are widely used to treat breast cancer, but docetaxel is more frequently used than paclitaxel, particularly in Japan. As far as we have been able to determine, there have been only two case reports describing the effectiveness of weekly paclitaxel therapy in patients, previously treated with docetaxel [19, 20]. And the objective of this study was to evaluate the efficacy, toxicity, and predictive factors for success of weekly paclitaxel therapy in MBC patients previously treated with docetaxel.

Patients and methods

A total of 308 patients with MBC were treated with weekly paclitaxel as salvage chemotherapy between January 1999 and October 2002 at the National Cancer Center Hospital. We retrospectively selected patients who fulfilled the following selection criteria as subjects for the present study: (1) docetaxel administered during prior chemotherapy for MBC; (2) adequate bone marrow and organ function (neutrophils >1500 μ^{-1}, AST <100 IU/l, ALT <100 IU/l, serum creatinine <2.0 mg/dl); (3) written informed consent before treatment. Patient treated with weekly paclitaxel plus trastuzumab combination was excluded.

Patients were intravenously (i.v.) infused with chorpheniramine maleate 10 mg and dexamethazsone 8 mg 30 min before the paclitaxel infusion. Paclitaxel 80 mg/m^2 was administered over a 1-h period weekly. Each 8-week cycle consisted of six consecutive weekly courses of treatment followed by a 2 week rest. Paclitaxel administration was repeated until there was evidence of disease progression or until unacceptable toxicity occurred. In the event of serious toxicity, treatment was withheld until recovery.

Patients with no bidimensionally measurable lesions were not eligible for objective response evaluation. Objective responses were evaluated according to WHO criteria [21]. Patients without measurable lesions were classified as not assessable (NA). Toxicity was evaluated according to National Cancer Institute Common Toxicity Criteria (NCI-CTC) ver 2.0.

Statistical analysis

The primary statistical analysis was performed to assess the effect of prior docetaxel response ('CR, PR, and NC' or 'PD') and interval between from the final infusion of docetaxel and disease progression. Since these two factors were highly correlated, we combined them and created a categorical variable (DTX profile) that has three levels: 'primary resistance,' 'secondary resistance' (short interval), and 'secondary resistance (long interval)', and the frequencies of response and non-response to weekly paclitaxel therapy were counted for each of these three levels of the DTX profile. The Cochran–Mantel–Haensxel test was performed for the 3×2 contingency table on the assumption that the DTX profile is an ordered categorical variable.

The secondary analysis consisted of a multivariate logistic regression to assess the effect of the following other factors on the response to paclitaxel therapy: DTX profile, performance status, number of organs involved, disease site, the number of prior regimens for MBC.

Time to progression was measured from the first day of treatment until disease progression or the final day of the follow-up period without disease progression, and overall survival time was measured from the first day of treatment until death or the final day of the follow-up period. Median time to progression and median overall survival were estimated by the Kaplan–Meier method. The statistical analysis was performed with SAS version 8.2 software (SAS Institute, Cary NC), and the significance level of the results was set at 0.05 level (two-sided).

Results

Patient characteristics

Of the 308 patients treated with weekly paclitaxel in our hospital, 96 patients had received prior docetaxel chemotherapy, and 14 patients of them were excluded based on the selection criteria described above: two patients on the basis of neutrophill count; 11 patients on the basis of liver function; one patient on the basis of serum creatinine value. Ultimately 82 of the 98 patients were included in the analysis. The patient characteristics are listed in Table 1. Median age was 54 years. Forty-one patients had received a regimen as adjuvant chemotherapy. The median number of organs involved was 2 (range: 1–5). The majority of the patients (67.1%) had visceral-dominant disease. Most of the patients (91.5%) had received two or more chemotherapy regimens for MBC. Seventy-five patients had received prior anthracycline-containing chemotherapy for MBC, and their median cumulative anthracycline exposure was 240 mg/m^2 (range: 80–480 mg/m^2). The median number of prior docetaxel cycles was 6 (range: 1–16). Most of the 82 patients (85.4%) had received docetaxel at a dose of 60 mg/m^2. The median cumulative docetaxel exposure in the study was 360 mg/m^2 (range: 120–960 mg/m^2). The median interval between the final infusion of docetaxel and the start of weekly paclitaxel therapy was 2.9 months (range: 0.5–23 months). Median follow-up time was 9.5 months, and the follow-up times ranged from 0.5–39 months.

Response

The total number of courses of weekly paclitaxel therapy was 909, and the median number of courses was 10

Table 1. Patient characteristics

	No. of patients (%)
Number	82
Age	
Median	54
ECOG performance status	
0	31
1	36
2	6
≧3	9
No. of organs involved	
1	20
2	31
3	19
≧4	12
Disease sites	
Primary lesion	6
Soft tissue metastasis	32
Lymph node metastasis	36
Liver metastasis	29
Lung metastasis	28
Pleural effusion	23
Bone metastasis	35
Brain metastasis	7
Disease pattern	
Visceral-dominant	54
Non-visceral dominant	28
No. of previous chemotherapy regimens	
1	7
2	57
≧3	18
Prior docetaxel chemotherapy	
Median number of courses	6
Range	1–16
Hormonal status (ER or PgR)	
Positive	38
Negative	31
Unknown	13

Abbreviations: ECOG: Eastern Cooperative Oncology Group; HER2: Human Epidermal Growth Factor Recepter type 2.

(range: 2–45). The response rate among all 82 patients was 19.5% (Table 2; 4 CR and 12 PR, 95% confidence interval (CI): 10.9–28.1%). Objective response rates according to previous docetaxel treatment profile are listed in Table 2. The differences in response rates between docetaxel treatment profiles (primary resistance, secondary resistance [Short interval], secondary resistance [Long interval]) were statistically significant ($p=0.0247$, Cochran–Mantel–Haenszel test). The results of the multivariate analyses did not suggested that any other factors affected the response to weekly paclitaxel treatment (Table 3). The median time to progression was 3.7 months (Figure 1; 95% CI: 2.75–4.72 months). Median overall survival was 9.4 months (Figure 1; 95% CI: 7.25–11.55 months).

Toxicity

A total of 909 courses in the 82 patients were assessable for toxic effects. The median cumulative dose of paclitaxel was 800 mg/m^2 (range: 160–3600 mg/m^2). The paclitaxel dosage was reduced in five patients due to toxicities: Grade 4 neutropenia in 2; Grade 3 fatigue in 1; Grade 3 diarrhea in 1; and Grade 3 neuropathy in 1. The toxicity profiles are listed in Table 4. Weekly paclitaxel treatment was generally well tolerated and manageable in an outpatient setting. Although grade 3 or 4 netropenia occurred in 10 patients (12.2%), no febrile neutropenia was observed. Neurosensory toxicity was observed in 51 patients (62.2%). No grade 4 non-hematological toxicity was reported, and there were no unexpected adverse reactions or treatment-related deaths.

Discussion

This study evaluated the efficacy and safety profile of weekly paclitaxel in docetaxel resistant MBC patients.

The definition of resistance to docetaxel referred to various definitions of drug resistance had been used in previous reports [12, 14, 18, 22]. The overall objective

Table 2. Objective response rate to weekly paclitaxel according to DTX profile

DTX profile	No. of patients	CR	PR	NC	PD	NA	RR (95% CI)
Primary resistance	24	0	2	10	10	2	8.3% (0–19.4%)
Secondary resistance	58	4	10	29	13	2	24.1% (13.1–35.1%)
Short interval	39	2	5	20	10	2	17.9% (5.9–30.0%)
Long interval	19	2	5	9	3	0	36.8% (15.1–58.5%)
Total no. of patients	82	4	12	39	23	4	19.5% (10.9–28.1%)

Cochran–Mantel–Haenszel test: $p = 0.027$ (primary resistance, short interval, long interval).
Abbreviations: CR: complete response; PR: partial response; NC: no change; PD: progressive disease; NA: not assessable; RR: response rate; CI: confidence interval; Short interval means ≦120 days between the final docetaxel infusion and disease progression. Long interval means > 120 days between the final docetaxel infusion and disease progression. All cases classified as 'primary resistance' experienced disease progression within 120 days of the final docetaxel infusion.

Table 3. Multivariate analyses of weekly paclitaxel response according to variables before weekly paclitaxel therapy (logistic regression model)

Variables before WPTX therapy	Odds ratio	95%CIs	*p* value
DTX profiles			
'Primary resistance':'Long interval'	0.131	0.022–0.773	0.0248
'Short interval':'Long interval'	0.368	0.101–1.339	0.1292
Performance status			
0–2:3–4	0.755	0.113–5.038	0.7716
Number of organs involved			
≧3:1–2	0.481	0.130–1.776	0.2723
Disease pattern			
Visceral:Non-visceral	1.276	0.345–4.720	0.7152
Number of prior regimens for MBC			
≧3:1–2	0.845	0.196–3.643	0.8212

Abbreviations: WPTX: weekly paclitaxel therapy.

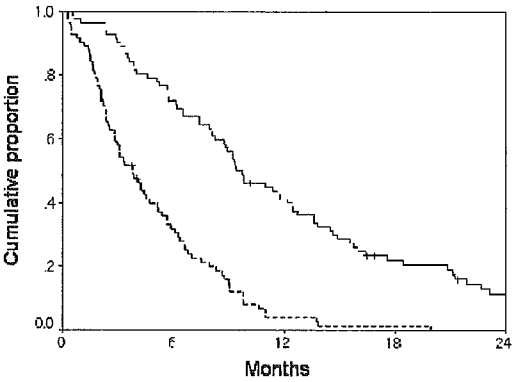

Figure 1. Kaplan–Meier analysis of time to progression (dots line) and overall survival (solid line). Vertical bars indicate censored cases.

Table 4. Maximum grade toxicity (% of patients)

	Maximum grade (NCI-CTC ver 2.0) % of patients			
	1	2	3	4
Leukopenia	36.6	30.5	8.5	0
Neutropenia	28	25.6	9.8	2.4
Anemia	36.6	14.6	4.9	0
Thrombocytopenia	1.2	0	0	0
Fatigue	23.1	3.7	1.2	0
Appetite loss	18.3	3.7	0	0
Nausea	23.2	0	1.2	0
Vomiting	14.6	0	1.2	0
Stomatitis	1.2	1.2	0	0
Diarrhea	3.7	0	1.2	0
Arthalgia/myalgia	4.9	2.4	0	0
HSR	7.3	3.7	0	0
Neurosensory	52.4	9.8	0	0

Abbreviations: HSR: hypersensitivity reactions.

response rate was 19.5%, and the response rate was higher in the secondary-resistance patients than in the primary-resistance patients (24.1 versus 8.3%), but the difference did not reach statistical significance. On the other hand, the interval between the final infusion of docetaxel and disease progression was a statistically significant predictor of response to the weekly paclitaxel. Previous studies on breast, ovarian and small-cell lung cancer described sensitive relapse were defined patients who relapse more than 3–6 months following completion of primary chemotherapy, and can be effectively retreated with same regimen or second-line chemotherapy [12, 22, 23]. Our result was attributable to the tumor biology of chemo-resistant as sensitive or refractory recurrence.

The results of study showed that weekly paclitaxel is modestly active in patients with docetaxel-resistant MBC and showed definite partial cross-resistance between paclitaxel and docetaxel, as reported previously in pre-clinical and clinical studies [9, 10, 17, 18]. Our study may be criticized for not a prospective study, but the overall objective response rate of 19.5% was almost the same as the overall response rates to docetaxel treatment in paclitaxel-resistant populations (18.1, 25%) [17, 18]. The response rate to weekly paclitaxel treatment in the primary docetaxel-resistance patients was poor than docetaxel treatment in the primary paclitaxel-resistance patients (8.3 versus 17.6, 20%) [17, 18]. In pre-clinical study, docetaxel exhibited greator cytotoxicity in paclitaxel-resistant cells [24]. Docetaxel has reported to be more active than paclitaxel against multi-drug resistance protein-expressing tumor [25]. Considering these findings it is reasonable that, there might be difference in the response in each primary resistant patient. We think that paclitaxel might not be useful in patients with primary docetaxel resistance.

In the present study, most patients were heavily treated MBC patients, and as a result the incidence of neutropenia (of any grade) was slightly higher than in previous studies of weekly paclitaxel in patients with anthracycline-refractory disease, however, the incidence of severe neutropenia (grade 3 or more) was comparable [15, 16]. By contrast, the incidence of paclitaxel-associated neurosensory toxicity was similar to its incidence in the previous studies [15, 16]. Therefore, weekly paclit-

axel was almost feasible treatment in outpatient setting, even if heavily treated MBC patients.

In conclusion, weekly paclitaxel therapy (80 mg/m^2) was modest effecacy in patient with docetaxel resistant MBC. However, the response rate of weekly paclitaxel therapy in primary resistance was clearly lower than that of patients with short and long interval. Therefore, weekly paclitaxel therapy should not be recommended for primary resistance patients with docetaxel.

References

1. Pivot X, Asmar L, Hortobagyi GN: The efficacy of chemotherapy with docetaxel and paclitaxel in anthracycline-reistant breast cancer. Int J Oncol 15: 381–386, 1999
2. Sparano JA: Taxanes for breast cancer: an evidence-based review of randomized phase II and phase III trials. Clin Breast Cancer 1: 32–40, 2000
3. Schiff PB, Fant J, Horwitz SB: Promotion of microtubule assembly in vitro by taxol. Nature 277: 665–667, 1979
4. Schiff PB, Horwitz SB: Taxol stabilizes microtubules in mouse fibroblast cells. Proc Natl Acad Sci USA 77: 1561–1565, 1980
5. Schiff PB, Horwitz SB: Taxol assembles tubuin in the absence of exogenous guanosine 5′-triphospahate or micro tubule-associated proteins. Biochemistry 20: 3247–3252, 1981
6. Jordan MA, Toso RJ, Wilson L: Mechanism of mitotic block and inhibition of cell proliferation by taxol at low concentration. Proc Natl Acad Sci USA 90: 9552–9556, 1993
7. Ringel I, Horwitz SB: Studies with RPR 56976 (Taxotere): a semisynthetic analogue of Taxol. J Natl Cancer Inst 83: 288–291, 1991
8. Haldar S, Basu A, Croce C: Bcl-2 is the guardian of microtuble integrity. Cancer Res 57: 229–233, 1997
9. Riou JF, Petitgenet O, Combeau C, Lavelle F: Cellular uptake and efflux of docetaxel and paclitaxel in P388 cell line. Proc Am Assoc Cancer Res 35: 385, 1994
10. Verweij J, Clavel M, Chevallier B: Paclitaxel (taxol) and docetaxel (taxotere): not simply two of a kind. Ann Oncol 5: 495–505, 1994
11. Alexandre J, Bleuzen P, Bonneterre J, Sutherland W, Misset JL, Guastalla J, Viens P, Faivre S, Chahine A, Spielman M, Bensmaine A, Marty M, Mahjoubi M, Cvitkovic E: Factors predicting for efficacy and safety of docetaxel in a compassionate use cohort of 825 heavily pretreated advanced breast cancer patients. J Clin Oncol 18: 562–573, 2000
12. Ando M, Watanabe T, Nagata K, Narabayashi M, Adachi I, Katsumata N: Efficacy of docetaxel 60 mg/m^2 in patients with metastatic breast cancer according to the status of anthracycline resistance. J Clin Oncol 19: 336–342, 2001
13. Adachi I, Watanabe T, Takashima S, Narabayashi M, Horikoshi N, Aoyama H, Taguchi T: A late phase II study of RP56976 (docetaxel) in patients with advanced or recurrent breast cancer. Br J Cancer 73: 210–216, 1996
14. Ravdin PM, Burris HAIII, Cook G, Eisenberg P, Kane M, Bierman WA, Mortimer J, Genevois E, Bellet RE: Phase II of docetaxel in advanced anthracycline-resistant or anthracenedione-resistant breast cancer. J Clin Oncol 13: 2879–2885, 1995
15. Seidman AD, Hudis CA, Albanel J, Tong W, Tepler I, Currie V, Moynahan ME, Theodoulou M, Gollub M, Baselga J, Norton L: Dose-dense therapy with weekly 1-hour paclitaxel infusions in the treatment of metastatic breast cancer. J Clin Oncol 16: 3353–3361, 1998
16. Perez EA, Vogel CL, Irwin DH, Kirshner JJ, Patel R: Multicenter phase II trial of weekly paclitaxel in woman with metastatic breast cancer. J Clin Oncol 19: 4216–4223, 2001
17. Lin YC, Chang HK, Wang CH, Chen JS, Liaw CC: Single-agent docetaxel in metastatic breast cancer patients pre-treated with anthracycline and paclitaxel: partial cross-resistance between paclitaxel and docetaxel. Anti-Cancer Drugs 11: 617–621, 2000
18. Valero V, Jones SE, Von Hoff DD, Boosner DJ, Mennel RG, Ravadin PM, Holmes FA, Rahman Z, Schottstaedt MW, Erban JK, Esparaza-Guerra L, Earnhart RH, Hortobagyi GN, BurrisIII HA: A phase II study of docetaxel in patients with paclitaxel-resitant metastatic breast cancer. J Clin Oncol 16: 3362–3368, 1998
19. Suzuma T, Sakurai T, Yoshimura G, Umemura T, Tamaki T, Naito Y: paclitaxel-induced remission in docetaxel refractory anthracycline-pretreated metastatic breast cancer. Anti-Cancer Drugs 11: 569–571, 2000
20. Ishitobi M, Shin E, Kikkawa N: Metastatic breast cancer with resistance to both anthracycline and docetaxel successfully treated with weekly paclitaxel. Int J Clin Oncol 6: 55–58, 2001
21. World Health Organization: WHO Handbook for reporting result of cancer treatment: offset publication 48, World Health Organization, Genova, 1979
22. Ardizzoni A, Manegolod C, Debruyne C, Gaafar R, Buchholz E, Smit EF, Lianes P, ten Velde G, Bosquee L, Legrand C, Neumaier C, King K: European organization for research and treatment of cancer (EORTC) 08957 phase II study of topotecan in combination with cisplatin as second-line treatment of refractory and sensitive small cell lung cancer. Clin Cancer Res 9: 143–150, 2003
23. Papadimitriou CA, Fountzilas G, Aravantios G, Kalofonos C, Moulopoulos LA, Briassoulis E, Gika D, Dimopoulos MA: Second-line chemotherapy with gemcitabine and cisplatin in paclitaxel-pretreated, platinum-sensitive ovarian cancer patients. A Hellenic Cooperative Oncology Group Study. Gynecol Oncol 92: 152–159, 2004
24. Sato S, Kigawa J, Kanamori Y, Itamachi H, Oishi T, Shimada M, Iba T, Naniwa J, Uegaki K, Terakawa N. Activity of docetaxel in paclitaxel-resistant ovarian cancer cells. Cancer Chemother Pharmacol 53: 247–252, 2004
25. Vanhoefer U, Cao S, Harstrick A, Seeber S, Rustum YM: Comparative antitumor efficacy of docetaxel and paclitaxel in nude mice bearing human tumor xenografts that overexpress the multidrug resistance protein (MRP) Ann Oncol 8: 1221–1228, 1997

Address for offprints and correspondence: Yasuhiro Fujiwara, Department of Medical Oncology, National Cancer Center Hospital, 5-1-1 Tsukiji, Chuo-ku, Tokyo 104-0045, Japan; *Tel.:* +81-3-3542-2511; *Fax:* +81-3-3542-3815; *E-mail:* yfujiwar@ ncc.go.jp

Bioelectromagnetics 27:51–57 (2006)

DNA Strand Breaks Are Not Induced in Human Cells Exposed to 2.1425 GHz Band CW and W-CDMA Modulated Radiofrequency Fields Allocated to Mobile Radio Base Stations

N. Sakuma,[1] Y. Komatsubara,[1] H. Takeda,[1] H. Hirose,[1]* M. Sekijima,[1] T. Nojima,[2] and J. Miyakoshi[3]

[1]*Research Division for Advanced Technology, Kashima Laboratory, Mitsubishi Chemical Safety Institute Ltd., Kamisu, Ibaraki, Japan*
[2]*Division of Electronics and Information Engineering, Graduate School of Hokkaido University, Sapporo, Japan*
[3]*Department of Radiological Technology School of Health Sciences, Faculty of Medicine, Hirosaki University, Hirosaki, Japan*

We conducted a large-scale in vitro study focused on the effects of low level radiofrequency (RF) fields from mobile radio base stations employing the International Mobile Telecommunication 2000 (IMT-2000) cellular system in order to test the hypothesis that modulated RF fields may act as a DNA damaging agent. First, we evaluated the responses of human cells to microwave exposure at a specific absorption rate (SAR) of 80 mW/kg, which corresponds to the limit of the average whole body SAR for general public exposure defined as a basic restriction in the International Commission on Non-Ionizing Radiation Protection (ICNIRP) guidelines. Second, we investigated whether continuous wave (CW) and Wideband Code Division Multiple Access (W-CDMA) modulated signal RF fields at 2.1425 GHz induced different levels of DNA damage. Human glioblastoma A172 cells and normal human IMR-90 fibroblasts from fetal lungs were exposed to mobile communication frequency radiation to investigate whether such exposure produced DNA strand breaks in cell culture. A172 cells were exposed to W-CDMA radiation at SARs of 80, 250, and 800 mW/kg and CW radiation at 80 mW/kg for 2 and 24 h, while IMR-90 cells were exposed to both W-CDMA and CW radiations at a SAR of 80 mW/kg for the same time periods. Under the same RF field exposure conditions, no significant differences in the DNA strand breaks were observed between the test groups exposed to W-CDMA or CW radiation and the sham exposed negative controls, as evaluated immediately after the exposure periods by alkaline comet assays. Our results confirm that low level exposures do not act as a genotoxicant up to a SAR of 800 mW/kg. Bioelectromagnetics 27:51–57, 2006. © 2005 Wiley-Liss, Inc.

Key words: DNA damage; radiofrequency radiation; alkaline comet assay; A172 cells; IMR-90 fibroblasts

INTRODUCTION

The rapid introduction of mobile telecommunication services over the last decade has drastically increased the amount of radiofrequency (RF) field irradiation frequencies and energies in our living environment. In order to continue stable growth and expansion of RF utilizations, it is necessary to investigate the possibility of any biological health effects of RF fields and to obtain reliable confirmation data with respect to safety. To achieve this, animal and cell culture studies of genotoxicity and carcinogenesis are very useful for providing risk assessment information. It is also important to examine the possible biological

Grant sponsor: NTT DoCoMo, Inc.

*Correspondence to: Hideki Hirose, Kashima Laboratory, Mitsubishi Chemical Safety Institute Ltd., 14 Sunayama, Kamisu, Ibaraki 314-0255, Japan. E-mail: h-hirose@ankaken.co.jp

Received for review 15 February 2005; Final revision received 11 July 2005

DOI 10.1002/bem.20179
Published online 10 November 2005 in Wiley InterScience (www.interscience.wiley.com).

effects of and obtain reliable data for 2-GHz band RF irradiation to facilitate the smooth deployment of the International Mobile Telecommunication 2000 (IMT-2000) cellular system. Here, we conducted a study that focused on the effects of a practical modulated signal for Wideband Code Division Multiple Access (W-CDMA) as well as a continuous wave (CW) at 2.1425 GHz, which corresponds to the middle frequency allocated to the downlink band of IMT-2000 from mobile radio base stations.

To date, most research has concentrated on the biological effects of the relatively high and short period RF irradiation from radio terminals. In contrast, only a few biological experiments related to the low level and long term exposure from radio base stations have been performed, since this exposure level is considered to be too small to have any biological effects on the humans. Moreover, in vitro studies using the single-cell gel electrophoresis (SCG) assay (comet assay), a sensitive technique for detecting DNA strand breaks [Singh et al., 1994, 1995; Tice et al., 2000], reported that RF fields did not induce direct genotoxic or carcinogenic effects [Malyapa et al., 1997; Vijayalaxmi et al., 2000; Li et al., 2001; McNamee et al., 2002a,b, 2003; Hook et al., 2004]. However, Phillips et al. [1998] reported that exposure of Molt-4 T-lymphoblastoid cells to an 836.55 MHz time-division multiple-access (TDMA) signal and 813.5625 MHz iDEN® signal at a specific absorption rate (SAR) of 2.4 mW/kg significantly decreased DNA damage, whereas the same iDEN signal at a SAR of 24 mW/kg significantly increased DNA damage. In addition, Lai and Singh [1995, 1996, 1997] reported that 2450 MHz pulsed and continuous microwave exposure at an average whole body SAR of 1.2 W/kg increased DNA damage in rat brain cells in vivo. Thus, it remains uncertain whether RF fields induce DNA damage, despite the large number of published studies regarding DNA damage after exposure to RF fields.

In the present study, human glioblastoma A172 cells were exposed to W-CDMA radiation at SARs of 80, 250, and 800 mW/kg and CW radiation at 80 mW/kg for 2 and 24 h, while normal human IMR-90 fibroblasts were exposed to both W-CDMA and CW radiations at a SAR of 80 mW/kg for the same time periods. The first objective of this study was to evaluate the responses of these human cells to microwave exposure at a SAR of 80 mW/kg, which corresponds to the limit of the average whole body SAR for general public exposure defined as a basic restriction in the International Commission on Non-Ionizing Radiation Protection [ICNIRP, 1998] guidelines. The second objective was to investigate whether CW and W-CDMA modulated signal RF fields at 2.1425 GHz, which corresponds to the center frequency of the IMT-2000, induced different levels of DNA damage.

MATERIALS AND METHODS

Cells and Culture Conditions

Human glioblastoma A172 cells were cultured in Dulbecco's modified Eagle medium (DMEM; Invitrogen, Tokyo, Japan) supplemented with 10% heat-inactivated fetal calf serum (FCS; Invitrogen), 100 U/ml penicillin, and 100 μg/ml streptomycin. Normal human IMR-90 fibroblasts from fetal lungs were grown in Eagle's minimal essential medium with Earle's balanced salts (Invitrogen) supplemented with 0.1 mM non-essential amino acids, 1.0 mM sodium pyruvate, 10% heat-inactivated FCS, 100 U/ml penicillin, and 100 μg/ml streptomycin. The two cell lines were obtained from the American Type Culture Collection (ATCC, Rockville, MD). All cell cultures were carried out in 100 mm diameter dishes at 37 °C in a humidified atmosphere of 5% CO_2. The doubling times of A172 and IMR-90 cells were 25.4 ± 2.1 and 38.9 ± 3.3 h, respectively, under these culture conditions.

Exposure System

The W-CDMA cellular system is one of the component systems of the IMT-2000 cellular system, and its frequency spectrum is shown in Figure 1. W-CDMA adopts Direct Sequence CDMA (DS-CDMA) and Frequency Division Duplex (FDD) as a multiple access and duplex scheme, respectively. The chip rate of the spread code of this system is 3.84 Mcps. A beam-formed RF exposure incubator employing a horn antenna, a dielectric lens, and a culture case in an anechoic chamber was developed for large-scale in vitro

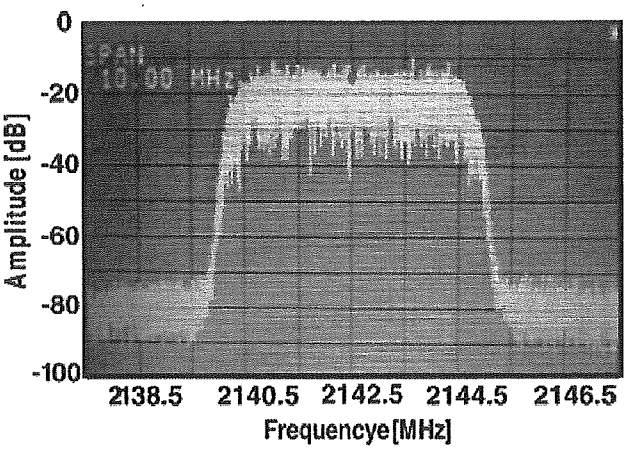

Fig. 1. Wideband Code Division Multiple Access (W-CDMA) frequency spectrum.

studies. A detailed description of the exposure system was published in Iyama et al. [2004]. Briefly, two identical RF field exposure incubators, one for RF field exposure and the other for sham exposure, were established in separate anechoic chambers, and a mechanical switch in a dummy box allows the selection of RF field exposure or sham exposure. This system allows simultaneous exposure of 49 (7 × 7 array) 35 mm culture dishes to a 2.1425 GHz RF electromagnetic field, which corresponds to the center frequency of the IMT-2000 down link band, with a uniform SAR distribution in the medium of all 49 culture dishes. The main unit for the cell exposure provides identical air to the two culture units through sealed ducts at the appropriate temperature (37 °C), CO_2 (5%), and humidity (>90%). The mean SAR of the culture fluid at the bottom of the 49 culture dishes used in the in vitro experiments was 175 mW/kg for an antenna input power of 1 W and the standard deviation of the SAR distribution was 59%. When only the inner 25 culture dishes (5 × 5 array) were evaluated, the mean SAR was 139 mW/kg for the same antenna input power and the standard deviation of the SAR distribution was 47%. Five dishes in the inner dish positions were used in this study.

Experimental Design

Human glioblastoma A172 cells were exposed to W-CDMA radiation at SARs of 80, 250, and 800 mW/kg and CW radiation at 80 mW/kg for 2 and 24 h, while human IMR-90 fibroblasts from fetal lungs were exposed to both W-CDMA and CW radiations at a SAR of 80 mW/kg for the same time periods. The exposure time of 2 and 24 h were chosen because DNA strand breaks increased in a time-dependent manner upon methyl methane sulfonate (MMS) treatment in our preliminary studies (data not shown). A172 glioblastoma or IMR-90 fibroblast cell cultures for RF field exposures were maintained in several 100 mm culture dishes from a common culture. Log phase cells were dissociated enzymatically, plated in 35 mm culture dishes and maintained for 48 h as a pre-culture. Next, the medium was exchanged for fresh medium, and the cell cultures were placed in the RF field exposure incubators. Five cultures were subjected to RF field or sham exposure for 2 or 24 h, respectively. The RF field exposures were processed in a blind manner. The air temperature was monitored for all cultures during the course of the sham and RF field exposures, and no significant variations were found. Empirical data collected over all the experiments demonstrated that the air temperatures within the cultures during the sham and RF field exposures were typically within 0.3 °C of each other at all times, and were within the range of 37.0 ± 0.5 °C once thermodynamic equilibrium was achieved within the exposure chamber at the highest SAR of 800 mW/kg for W-CDMA radiation. The temperatures of the culture media during the sham and RF field exposures cultures typically remained within 0.3 °C. Specifically, the temperature ranges were 37.0 ± 0.3, 37.0 ± 0.1, and 37.0 ± 0.1 °C at the SARs of 800, 250, and 80 mW/kg for W-CDMA radiation, respectively. Other cultures were treated with 0, 2, 4, and 20 μg/ml MMS as positive controls in a conventional incubator. Furthermore, 20 μg/ml MMS was used as a positive control in every RF field exposure experiment.

Alkaline Comet Assay

After the exposure, the RF field, sham and 20 μg/ml MMS samples were processed for the alkaline comet assay as described by Singh et al. [1994, 1995]. Briefly, the cells were washed, resuspended in Ca^{2+}- and Mg^{2+}-free phosphate buffered saline at a concentration of 1×10^5 cells/ml, and mixed with 1% low melting point agarose at a ratio of 1:5. The mixtures were immediately layered onto slides and placed in a refrigerator to allow the mixture to gel. Next, the slides were transferred to a chamber containing lysis buffer (Trevigen, Gaithersburg, MD), and treated with 1 mg/ml proteinase K solution (Qiagen, Tokyo, Japan) at 37 °C for 2 h. The slides were then rinsed in electrophoresis buffer (pH 13; 300 mM NaOH, 1 mM EDTA) for 10 min, subjected to electrophoresis at 22 V and 300 mA for 30 min, dehydrated in 70% ethanol for 10 min and air dried overnight.

The samples were analyzed after staining with 10 μg/ml ethidium bromide. Images were acquired with an Olympus fluorescence microscope using a 20× objective lens and 520–540 nm excitation from a 100 W mercury lamp. All comet images were acquired with a cooled color CCD camera, and at least 100 comets from each of the five replicate cultures were analyzed using the Komet 5 imaging system (Kinetic Imaging Ltd., NC). The comet head and tail regions were defined manually. Tail length was defined as the distance from the leading edge of the comet head to the leading edge of the tail. Tail DNA was calculated as the relative fluorescence intensity in the comet tail region to that in the entire comet. Olive tail moment was calculated as the tail DNA multiplied by the distance between the centers of gravity of the head and tail regions [Olive et al., 1990].

Statistical Analysis

The DNA strand breaks obtained with the alkaline comet assay were analyzed by Student's *t*-test or Welch's *t*-test using the data for the sham exposed samples, the RF field exposed samples and the positive

(20 μg/ml MMS treatment) controls for each of the three end points (Olive tail moment, tail DNA, and tail length). Student's *t*-test was performed if the variance was homogeneous, while Welch's *t*-test was used if the variance was heterogeneous. A *P*-value of less than .05 was considered statistically significant.

RESULTS

DNA Strand Breaks After MMS Treatment

MMS treatment was used as both a positive control and to assess the sensitivity of the method used to detect DNA damage. A172 and IMR-90 cells were cultured with MMS at concentrations of 0, 2, 4, and 20 μg/ml for 2 or 24 h. The lowest detectable dose of each parameter (Olive tail moment, tail DNA, or tail length) was 2 or 4 μg/ml MMS for both cell lines used in the study (Fig. 2). For A172 cells, the Olive tail moment and tail length after culture with 2 μg/ml MMS for 2 h were greater than the background (0 μg/ml MMS), but the difference was not significant. For IMR-90 cells, the tail length after culture with 2 μg/ml MMS for 24 h did not differ significantly from the background (0 μg/ml MMS).

DNA Strand Breaks After Exposure to RF Field at 80 mW/kg

A172 cell cultures were exposed to W-CDMA or CW radiation at a SAR of 80 mW/kg for 2 or 24 h. Experiments under the same RF field exposure conditions were repeated three times, and five different cultures were used in each experiment. The pooled experimental data (15 different cultures) for the same system and duration of RF field exposure are summarized in Table 1. No significant differences were observed between any of the RF field exposure groups and the sham exposed controls for any of the parameters examined, in either the 2.1425 GHz W-CDMA or CW RF field experiments. MMS, the positive control agent, induced a significant and noticeable increase in DNA migration in all experiments.

IMR-90 cells were exposed to W-CDMA or CW radiation at a SAR of 80 mW/kg for 2 or 24 h, and the results are summarized in Table 2. All the comet parameters were small in these experiments. No statistically significant differences were observed between any of the RF field exposure groups and the sham exposed controls for any of the parameters examined, in

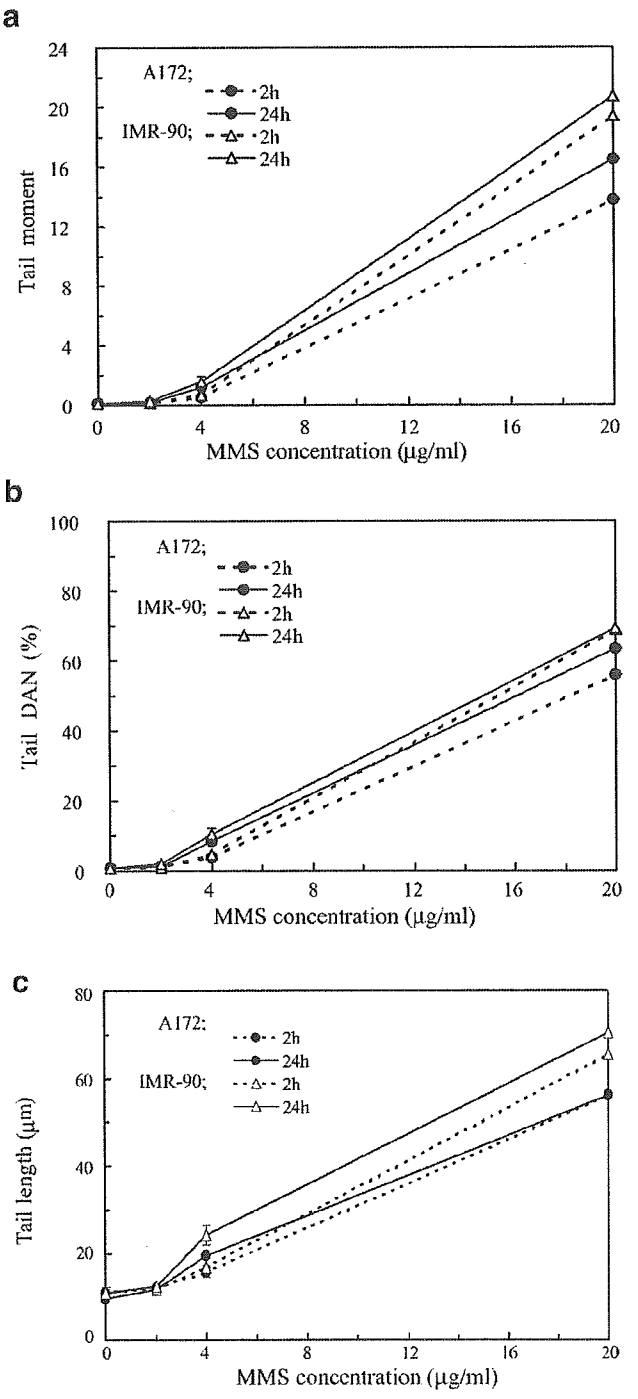

Fig. 2. DNA strand breaks in A172 and IMR-90 cells cultured with methyl methane sulfonate (MMS) at 0, 2, 4, and 20 μg/ml for 2 or 24 h. The Olive tail moment (**a**), tail DNA (**b**), and tail length (**c**) were measured immediately after the treatment. The data points represent the means ± SD of three independent cultures. After treatment of A172 cells with 2 μg/ml MMS for 2 h, the tail moment and tail length are not significantly different from the background (0 μg/ml MMS). However, all three comet parameters differ significantly from the background after treatment with 4 μg/ml MMS ($P < .01$). After treatment of IMR-90 cells with 2 μg/ml MMS for 24 h, the tail length is not significantly different from the background. However, all three comet parameters differ significantly from the background after treatment with 4 μg/ml MMS ($P < .01$).

TABLE 1. Comparison of Comet Parameters in A172 Cells Exposed to 2.1425 GHz Radiofrequency (RF) Radiation and Sham Radiation

System	Specific absorption rate (SAR) (mW/kg)	Time (h)	Tail moment		Tail DNA (%)		Tail length (μm)	
			RF	Sham	RF	Sham	RF	Sham
Wideband Code Division Multiple Access (W-CDMA)	800	2	0.20 ± 0.060	0.19 ± 0.060	1.71 ± 0.525	1.64 ± 0.538	11.56 ± 2.112	11.20 ± 2.329
		24	0.16 ± 0.037	0.16 ± 0.031	1.42 ± 0.367	1.42 ± 0.334	11.15 ± 2.223	10.97 ± 2.316
	250	2	0.26 ± 0.063	0.27 ± 0.083	2.23 ± 0.583	2.28 ± 0.685	12.03 ± 1.625	12.04 ± 1.656
		24	0.26 ± 0.059	0.27 ± 0.059	2.30 ± 0.607	2.38 ± 0.632	12.11 ± 1.581	12.21 ± 1.512
	80	2	0.26 ± 0.043	0.27 ± 0.029	2.28 ± 0.341	2.33 ± 0.241	13.36 ± 1.276	13.25 ± 1.645
		24	0.27 ± 0.050	0.29 ± 0.054	2.38 ± 0.432	2.50 ± 0.358	13.29 ± 1.426	13.29 ± 1.559
Continuous wave (CW)	80	2	0.24 ± 0.168	0.23 ± 0.150	2.10 ± 1.636	2.01 ± 1.407	10.07 ± 3.097	9.93 ± 3.226
		24	0.25 ± 0.174	0.24 ± 0.167	2.24 ± 1.725	2.14 ± 1.672	10.34 ± 2.701	9.92 ± 3.116
MMS[a]		2	—	16.31 ± 5.095*	—	62.32 ± 8.664*	—	49.44 ± 9.859*
		24	—	19.44 ± 4.752*	—	67.65 ± 7.889*	—	53.51 ± 8.120*

Each data point represents the mean ± the standard deviation (SD) for 15 cultures. One hundred cells (50 cells from two spots) were measured for each culture at each experiment.
[a]Other cultures were treated with 20 μg/ml methyl methane sulfonate (MMS) for positive control in every RF exposure experiment; mean ± the SD for three experiments (cultures).
*Significance ($P < .001$) from the sham control.

TABLE 2. Comparison of Comet Parameters in IMR-90 Cells Exposed to 2.1425 GHz RF Radiation and Sham Radiation

System	SAR (mW/kg)	Time (h)	Tail moment		Tail DNA (%)		Tail length (μm)	
			RF	Sham	RF	Sham	RF	Sham
W-CDMA	80	2	0.14 ± 0.076	0.14 ± 0.086	1.35 ± 0.842	1.36 ± 0.894	9.06 ± 3.877	8.89 ± 4.218
		24	0.15 ± 0.139	0.11 ± 0.062	1.38 ± 1.104	1.15 ± 0.653	8.72 ± 4.296	8.16 ± 4.463
CW	80	2	0.09 ± 0.014	0.09 ± 0.015	0.75 ± 0.091	0.76 ± 0.108	7.57 ± 2.446	7.74 ± 2.138
		24	0.09 ± 0.019	0.09 ± 0.017	0.75 ± 0.195	0.77 ± 0.169	7.41 ± 1.522	7.94 ± 1.729
MMS[a]		2	—	17.13 ± 1.519*	—	66.76 ± 3.320*	—	58.44 ± 7.545*
		24	—	19.52 ± 2.665*	—	70.74 ± 3.289*	—	57.75 ± 9.119*

Each data point represents the mean ± the SD for 15 cultures. One hundred cells (50 cells from two spots) were measured for each culture at each experiment.
[a]Other cultures were treated with 20 μg/ml MMS for positive control in every RF exposure experiment; mean ± the SD for three experiments (cultures).
*Significance ($P < .001$) from the sham control.

either the 2.1425 GHz W-CDMA or CW RF field experiments. MMS induced a significant increase in DNA migration in all experiments.

DNA Strand Breaks After Exposure to RF Field at 250 or 800 mW/kg

A172 cell cultures were exposed to W-CDMA radiation at a SAR of 250 or 800 mW/kg for 2 or 24 h, and the results are summarized in Table 1. No significant differences were observed between any of the W-CDMA exposure groups and the sham exposed controls for any of the parameters examined at an average SAR of 250 or 800 mW/kg. MMS induced a significant increase in DNA migration in all experiments.

DISCUSSION

The comet assay is a simple and sensitive assay that is capable of measuring and identifying DNA strand breaks at the cellular level [Singh et al., 1995; Tice et al., 2000]. In both cell lines, treatment with 20 μg/ml MMS for 2 and 24 h induced increases in all three comet parameters (Olive tail moment, tail DNA, and tail length), although the survival of the cells did not differ from the background after either 2 or 24 h of treatment (A172: 2 h, 91.0% vs. 96.0%; 24 h, 91.0% vs. 98.8%; IMR-90: 2 h, 93.7% vs. 96.3%; 24 h, 90.6% vs. 95.9%).

Figure 2 shows the DNA strand breaks in A172 and IMR-90 cells after culture with different concentrations of MMS for 2 or 24 h. In our comet assay protocol, the cell suspensions and low melting point agarose layered onto slides were treated with 1 mg/ml proteinase K to increase the sensitivity, since Singh et al. [1995] reported that proteinase K treatment of cells allowed the detection of DNA strand breaks in human lymphocytes irradiated with low doses of γ rays. Our results further confirmed that proteinase K treatment of the cells raised the sensitivity of detection of DNA strand breaks. None of the measured comet parameters in comet assays for A172 or IMR-90 cells were significantly higher than the background after treatment with 10 μg/ml MMS without proteinase K treatment (data not shown). However, all the comet parameters were significantly above the background after treatment of both cell lines with 4 μg/ml MMS followed by 1 mg/ml proteinase K (Fig. 2). Thus, these results confirmed that the comet assay performed in this study could detect DNA strand breaks with high sensitivity.

In the present study, we analyzed the human A172 and IMR-90 cells for DNA strand breaks after exposure to RF signals for 2 or 24 h. A172 cells were exposed to W-CDMA radiation at SARs of 80, 250, and 800 mW/kg and CW radiation at 80 mW/kg, while IMR-90 cells were exposed to both W-CDMA and CW radiations at a SAR of 80 mW/kg. The exposures to RF radiation were carried out in a blind manner so that it was not possible to identify the RF field and sham exposed samples. Three comet parameters (Olive tail moment, tail DNA, and tail length) were obtained for each comet scored by image analysis, after averaging the responses across different populations of cells within each culture. For all the RF field exposure conditions, no significant differences in the DNA strand breaks were observed between the test groups exposed to W-CDMA or CW radiation and the sham exposed negative controls when the samples were processed immediately after the exposure periods by the alkaline comet assay. In our previous study, we showed that exposure to 2.1425 GHz CW and W-CDMA modulated RF signals at a SAR of up to 800 mW/kg did not alter the cell proliferation ratio or cell cycle phase in four human cell lines, including A172 and IMR-90 cells. Furthermore, none of the CW and W-CDMA modulated RF signals tested had any effects on the expression profiles of genes encoding proteins related to the cell cycle, cell proliferation, cell death, apoptosis, etc. (data not shown).

Our results confirm that exposure to W-CDMA and CW 2.1425 GHz microwaves for 2 and 24 h did not act as a genotoxicant at the limit of the average whole body SAR level defined in the ICNIRP guidelines.

ACKNOWLEDGMENTS

The authors thank Ms. Naoko Kaji for her technical assistance during this research.

REFERENCES

Hook GJ, Zhang P, Lagroye I, Li L, Higashikubo R, Moros EG, Straube WL, Pickard WF, Baty JD, Roti Roti JL. 2004. Measurement of DNA damage and apoptosis in Molt-4 cells after in vitro exposure to radiofrequency radiation. Radiat Res 161:193–200.

ICNIRP. 1998. Guidelines for limiting exposure to time varying electric, magnetic and electromagnetic fields (up to 300 GHz). Health Phys 74:494–522.

Iyama T, Ebara H, Tarusawa Y, Uebayashi S, Sekijima M, Nojima T, Miyakoshi J. 2004. Large-scale in vitro experiment system for 2 GHz-exposure. Bioelectromagnetics 25:599–606.

Lai H, Singh NP. 1995. Acute low-intensity microwave exposure increases DNA single-strand breaks in rat brain cells. Bioelectromagnetics 16:207–210.

Lai H, Singh NP. 1996. Single- and double-strand DNA breaks in rat brain cells after acute exposure to radiofrequency electromagnetic radiation. Int J Radiat Biol 69:513–521.

Lai H, Singh NP. 1997. Melatonin and a spin-trap compound block radiofrequency electromagnetic radiation-induced DNA strand breaks in rat brain cells. Bioelectromagnetics 18: 446–454.

Li L, Bisht KS, LaGroye I, Zhang P, Straube WL, Moros EG, Roti Roti JL. 2001. Measurement of DNA damage in mammalian cells exposed in vitro to radiofrequency fields at SARs of 3–5 W/kg. Radiat Res 156:328–332.

Malyapa RS, Ahern EW, Straube WL, Moros EG, Pickard WF, Roti Roti JL. 1997. Measurement of DNA damage after exposure to electromagnetic radiation in the cellular phone communication frequency band (835.62 and 847.74 MHz). Radiat Res 148:618–627.

McNamee JP, Bellier PV, Gajda GB, Miller SM, Lemay EP, Lavallee BF, Marro L, Thansandote A. 2002a. DNA damage and micronucleus induction in human leukocytes after acute in vitro exposure to a 1.9 GHz continuous-wave radiofrequency field. Radiat Res 158:523–533.

McNamee JP, Bellier PV, Gajda GB, Lavallee BF, Lemay EP, Marro L, Thansandote A. 2002b. DNA damage in human leukocytes after acute in vitro exposure to a 1.9 GHz pulse-modulated radiofrequency field. Radiat Res 158:534–537.

McNamee JP, Bellier PV, Gajda GB, Lavallee BF, Marro L, Lemay EP, Thansandote A. 2003. No evidence for genotoxic effects from 24 h exposure of human leukocytes to 1.9 GHz radiofrequency fields. Radiat Res 159:693–697.

Olive PL, Banath JP, Durand RE. 1990. Heterogeneity in radiation-induced DNA damage and repair in tumor and normal cells using the "comet" assay. Radiat Res 122:86–94.

Phillips JL, Ivaschuk O, Ishida-Jones T, Jones RA, Compbell-Beachler M, Haggren W. 1998. DNA damage in Molt-4 T-lymphoblastoid cells exposed to cellular telephone radiofrequency fields in vitro. Bioelectrochem Bioenerg 45:103–110.

Singh NP, Stephens RE, Schneider EL. 1994. Modification of alkaline microgel electrophoresis for sensitive detection of DNA damage. Int J Radiat Biol 66:23–28.

Singh NP, Graham MM, Singh V, Khan A. 1995. Induction of DNA single-strand breaks in human lymphocytes by low dose of γ-rays. Int J Radiat Biol 68:563–569.

Tice RR, Agurell E, Anderson D, Burlinson B, Hartmann A, Kobayashi H, Miyamae Y, Rojas E, Ryu JC, Sasaki YF. 2000. Single cell gel/comet assay: Guidelines for in vitro and in vivo genetic toxicology testing. Environ Mol Mutagen 35: 206–221.

Vijayalaxmi, Leal BZ, Szilagyi M, Prihoda TJ, Meltz ML. 2000. Primary DNA damage in human blood lymphocytes exposed in vitro to 2450 MHz radiofrequency radiation. Radiat Res 153:479–486.